Multivariate curve resolution methods and the design of experiments.

Mathias Sawall[a], Christoph Kubis[b], Henning Schröder[a,b], Denise Meinhardt[a,b], Detlef Selent[b], Robert Franke[c,d], Alexander Brächer[c], Armin Börner[b], Klaus Neymeyr[a,b]

[a] *Universität Rostock, Institut für Mathematik, Ulmenstrasse 69, 18057 Rostock, Germany*
[b] *Leibniz-Institut für Katalyse, Albert-Einstein-Strasse 29a, 18059 Rostock*
[c] *Evonik Industries AG, Paul-Baumann Straße 1, 45772 Marl, Germany*
[d] *Lehrstuhl für Theoretische Chemie, Ruhr-Universität Bochum, 44780 Bochum, Germany*

Abstract

A major problem of multivariate curve resolution methods is the underlying non-uniqueness of the pure component decompositions. This raises the question how a chemical experiment should be designed so that the solution ambiguity is as small as possible. Changes of the reaction conditions belong to the possible variations whereas for a fixed chemical reaction system the pure component spectra appear to be unchangeable.

The paper investigates and discusses the possibility to design a chemical experiment in a way that minimizes the ambiguity of the factorization. The analysis identifies regions of the spectra that are responsible for a small ambiguity. Certain sources are identified that are responsible for an increased ambiguity by means of an a posteriori analysis. This results in recommendations how to construct spectral measurements incorporating a reduced factorization ambiguity. Furthermore, lower bounds on an unavoidable base level of ambiguity are specified under the constraint of fixed reactants. The problem analysis is accompanied by investigations of several experimental data sets.

Key words: multivariate curve resolution, ambiguity, design of experiments.

1. Introduction

Design of experiments (DoE) is a methodology for the planning and the statistical analysis of experiments. The aim is to detect and to explain changes of the extractable system information with respect to changes of the experimental conditions. Mainly with the background of agricultural applications, the statistician R. Fisher developed the principles of DoE in 1926 [1] and later in 1935 in his book entitled *Design of Experiments* [2]. Today, DoE is a very important and widely used method that supports scientists in the systematical development of statistical experimental designs.

This paper deals with the *related* problem to which extent the uncertainty of the results of multivariate curve resolution (MCR) methods for the pure component decomposition of series of spectra can be reduced by changing the experimental conditions. Conditions for reducing the rotational ambiguity in MCR computations have a history for more than two decades. Tauler and coworkers showed between 1993 and 1995 how additional constraints as selectivity and local rank assumptions as well as multiset and multiway data can help to reduce ambiguity [3, 4, 5]. At the same time Manne [6] published his influential resolution theorems where such conditions were confirmed. On the side of method development these findings led among others to evolving factor analysis method of Maeder [7], the window factor analysis by Malinowski [8] and the Heuristic Evolving Latent Projections (HELP) by Kvalheim and Liang [9]. Further, Paatero and coworkers developed the Positive Matrix Factorization (PFM) method for factorizations of air source apportionment data [10, 11]. All these methods exploit the knowledge where certain components of a mixture exist or are absent, and where they contribute or do not contribute to the measured signal. Further, any zero pattern in the spectral mixture data or the pure component factors contains a valuable information on the pure components. All these criteria define starting points for applying DoE techniques for decreasing rotational ambiguities for the individual analysis of single data sets and also for the simultaneous analysis for multiset and multiway data. The importance of well-designed chemical experiments for the subsequent numerical analysis of the spectral data has been pointed out by many authors; for the context of operando spectroscopy in homogeneous catalysis we refer to Garland [12].

The uncertainties in the solution of MCR problems due to the *rotational ambiguity* can be displayed in the form of feasible bands or in the low-dimensional form by the so-called Area of Feasible Solutions (AFS). Our analysis does not include an application of DoE in the sense of statistical methods for information extraction. Instead, we investigate the problem of an uncertainty reduction by analyzing conditions how chemical experiments should be designed in order to reduce the rotational ambiguity. The analysis also considers the question which spectral windows (of the series of spectra) are decisive for the extent of the solution ambiguity. We derive by means of an a posteriori analysis conditions and recommendations of how to design a chemical experiment and how to plan the spectral measurements in an a priori

way so that the spectroscopic observation and the subsequent MCR analysis can yield reliable pure component factors with a reduced uncertainty. The recommended changes of the experimental conditions can concern the selection of the solvent, changes in temperature or pressure, the presence or non-presence of perturbations together with the question of a spectral background treatment and so on.

1.1. The MCR problem and its solution ambiguity

We consider the MCR problem for a $(k\times n)$-matrix D whose k rows are formed by a series of spectra. Each spectrum has n spectral channels. The aim is to determine the pure component factors, namely a matrix of concentration profiles $C \in \mathbb{R}^{k\times s}$ and a second matrix $S \in \mathbb{R}^{n\times s}$ of the pure component spectra, with

$$D = CS^T + E. \tag{1}$$

Ideally the residual matrix E is the zero matrix or otherwise elementwise close to zero. The number s denotes the number of the pure components. The factorization problem, i.e. to compute for an experimentally measured (nonnegative) matrix D the two nonnegative matrix factors C and S so that (1) is satisfied for neglectable E, cannot be expected to have a unique solution. Naturally, we ignore simultaneous permutations of the columns of C and S and comparable positive column scaling of these matrices as trivial sources of a solution ambiguity. Instead the non-trivial non-uniqueness, the so-called rotational ambiguity, is a major problem [8, 13, 14, 15, 16]. The AFS, see Section 2.1 for details, is a low-dimensional representation of the possible columns of either C or S and has extensively been studied in recent years [17, 18, 19, 20, 21, 22, 23, 24, 25].

The bilinear Lambert-Beer model (1) determines the two pure component factors as the two influential quantities to form the mixture data; we ask how to change the reaction system with the aim of a reduction of the rotational ambiguity. Reasonably, a change of the reactants of the chemical reaction system makes no sense and hence the factor S of the pure component spectra is not subject to any change. Nevertheless, we discuss the effect of isolated peaks or frequencies with partly non-absorbing components on the AFS. In contrast to this, changes of the reaction conditions, which do not lead to new chemical products, can considerably change the concentration profiles of the pure components that form the columns of C. Additionally, repeated experiments with very different concentration values can also reduce the ambiguity of the MCR solutions.

The questions of the rotational ambiguity of MCR solutions and techniques for an ambiguity reduction (e.g. by duality arguments [26, 27, 28]) are discussed in many of the publications referenced above. Our analysis has some relations to the works of Manne [6] as well as Rajkó and coworkers [29]. The two papers are widely known and are important concerning the uniqueness or partial uniqueness of MCR solutions for bivariate data. A key-principle in [29] is the *data-based uniqueness* whereas in [6] principles of a *profile-based uniqueness* in selective windows are developed. In these two works the focus is on unique solutions. In contrast to this, we here analyze a *reduction* of the AFS-sets of solutions under changing conditions. For the extreme case of a reduction up to uniqueness our results are consistent with those in [29].

In general, unique pure components can only be determined in special cases for experimental spectral data (however model problems can be constructed that show such a singular behavior). Such a situation can exist if, in the words of Manne, *selective regions* can be determined in the spectra. These selective regions contain only signals of one component and can help to extract the entire pure component spectrum of this component. The existence of selective regions is a special favorable situation in experimental spectral data and appears to be unlikely in the presence of noise, background spectra or distorted baselines.

Organization of the paper: The central second section of the paper treats the ambiguity reduction problem in a geometrical manner by using Borgen plots (case $s = 3$) and its generalization to higher numbers of components ($s > 3$) by using the polygons/polyhedra FIRPOL and INNPOL for the AFS construction. Some of the presented results are similar to statements that have been gained in [29]. In Section 3 guiding principles are developed for experimental conditions that lead to relatively small AFS-sets. In Section 4 we discuss lower bounds on the rotational ambiguity of MCR factorizations under the assumption of fixed pure component spectra. Finally, Section 5 illustrates the application of the theoretical results to some data sets of chemical three-component systems. If the reader is not familiar with Borgen plots and their underlying mathematical theory, then we recommend to skip the theoretical second section and to continue with the recommendation for an ambiguity reduction in Section 3 and their application demonstrations in section 4.

2. Borgen plots and rotational ambiguity in AFS constructions

Borgen plots [17, 18] and their crucial polygons INNPOL and FIRPOL are the decisive tools for the analysis in this sections; see Eq. (2), for the mathematical definition of these polygons. First, FIRPOL is the set of all points which represent nonnegative profiles. Hence, any acceptable solution (concentration profile or spectrum) must be

represented by a point in FIRPOL. If small negative components are acceptable, then the representing point can leave FIRPOL but must be close to its surface. Second, the polygon INNPOL is contained in FIRPOL and is the convex hull of all points that represent either the columns or the rows of the spectral data matrix. The polygons INNPOL and FIRPOL are the basis for the construction of the so-called Borgen plots, see [17].

Our analysis starts with the uniqueness condition that a vertex of INNPOL is located on the boundary of FIRPOL. Then we discuss conditions whether or not additional mixture spectra (namely a row of D) enlarges the size of the polygon INNPOL or decreases the size of FIRPOL. Both changes result in a reduction of the rotational ambiguity since the triangle (simplex) rotation process in the geometric Borgen plot construction works under stronger constraints for the possible locations of the vertices of the triangles/simplices. Next we introduce the AFS and its geometric construction by Borgen plots with the notation following [28, 30].

2.1. Borgen plots

The starting point is the spectral data matrix D and its (approximate) nonnegative factors C and S according to (1). The truncated singular value decomposition (SVD) $U\Sigma V^T = D$ provides by the left (resp. right) singular vectors a basis for the representation of the factor C (resp. S). The expansion coefficients with respect to these bases are collected in a regular matrix $T \in \mathbb{R}^{s\times s}$ so that the matrix factors have the forms $C = U\Sigma T^{-1} \geq 0$ and $S^T = TV^T \geq 0$, see e.g. [31, 8, 14]. [1] The rotational ambiguity expresses the fact that usually a continuum of $s\times s$ matrices T exists so that $C, S \geq 0$. MCR methods aim at determining only a single factorization and typically require additional constraints and assumptions. There is no guarantee that the chemically correct solution can be determined. An alternative and assumption-free approach is to compute the set of all nonnegative factorizations of D, to analyze all these solutions and finally to try to choose the true solutions. Practically, there is no necessity to consider the set of all pairs of nonnegative matrices (C, S). Instead, the sets of all possible *first columns* of either C or S can be considered that arise in a nonnegative factorization $D = CS^T$. These columns can be represented in a low-dimensional way by the possible first rows of T (in order to represent the factor S) or the possible first columns of T^{-1} (to represent the factor C). Together with a proper normalization that fixes the first column of T to the all-ones vector (see [21] for a justification of this normalization by the Perron-Frobenius spectral theory of nonnegative matrices) we consider matrices T of the form

$$T = \begin{pmatrix} 1 & x_1 & \cdots & x_{s-1} \\ 1 & & & \\ \vdots & & W & \\ 1 & & & \end{pmatrix}.$$

The AFS for the factor S reads with $x = (x_1, \ldots, x_{s-1})^T$ and W

$$\mathcal{M}_S = \{x \in \mathbb{R}^{s-1} : \text{ exists } W \in \mathbb{R}^{(s-1)\times(s-1)} \text{ such that } \operatorname{rank}(T) = s \text{ and } C, S \geq 0\}.$$

Its pendant for C is denoted $\mathcal{M}_C$; cf. Eq. (5) in [28]. Various methods for the geometric construction or numerical computation of the AFS are available, see among others [17, 18, 19, 20] or the review works [24, 25]. Here the focus is on geometric constructions of the AFS in terms of the so-called Borgen plots [17, 18, 22]. To this end we need certain polyhedra, namely the two polyhedra FIRPOL $\mathcal{F}_S$ and $\mathcal{F}_C$ (the name derives from *first polygon*) and the polyhedra INNPOL $\mathcal{I}_S$ and $\mathcal{I}_C$ (the name derives from *inner polygon* as FIRPOL includes INNPOL). For the important case of a three-component system with $s = 3$ the polyhedra are (planar) polygons. The polyhedra are defined as follows

$$\begin{aligned} \mathcal{F}_S &= \left\{ x \in \mathbb{R}^{s-1} : \; V \begin{pmatrix} 1 \\ x \end{pmatrix} \geq 0 \right\}, & \mathcal{I}_S &= \operatorname{convhull}(\{a_i,\ i = 1, \ldots, k\}), \\ \mathcal{F}_C &= \left\{ y \in \mathbb{R}^{s-1} : \; U\Sigma \begin{pmatrix} 1 \\ y \end{pmatrix} \geq 0 \right\}, & \mathcal{I}_C &= \operatorname{convhull}(\{b_j,\ j = 1, \ldots, n\}). \end{aligned} \tag{2}$$

Therein the convhull operator generates the convex hull of either the k vectors a_i or the n vectors b_j. These vectors are the normalized vectors of expansion coefficients of the rows and columns of D with respect to the bases of its left and right singular vectors

$$a_i = \frac{(U\Sigma)^T(2:s, i)}{(U\Sigma)^T(1, i)}, \quad i = 1, \ldots, k, \qquad \text{and} \qquad b_j = \frac{(V(j, 2:s))^T}{V(j, 1)}, \quad j = 1, \ldots, n, \tag{3}$$

[1] We use the matrix T and also mark the transpose of matrix by a superscript T.

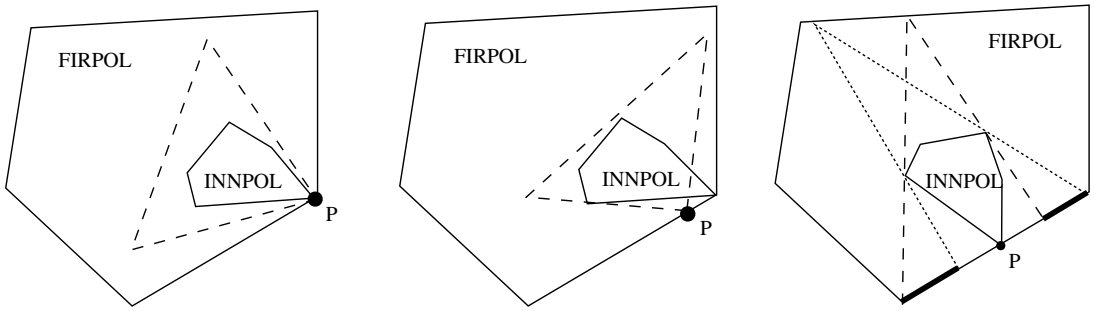

Figure 1: Three geometric arrangements in which a vertex of INNPOL touches the boundary of FIRPOL. Left: The point of contact P is a vertex of FIRPOL. Any Borgen triangle (a typical triangle is drawn by dashed lines) between INNPOL and FIRPOL necessarily has one of its vertices in P. A single and unique pure component is determined. This point cannot be moved to its close neighborhood. This is illustrated by the centered plot where an edge of the dashed triangle intersects INNPOL. Right: If the point P is located on an edge of FIRPOL and not in a vertex, then the AFS typically has two line-shaped subsets (marked by the bold lines).

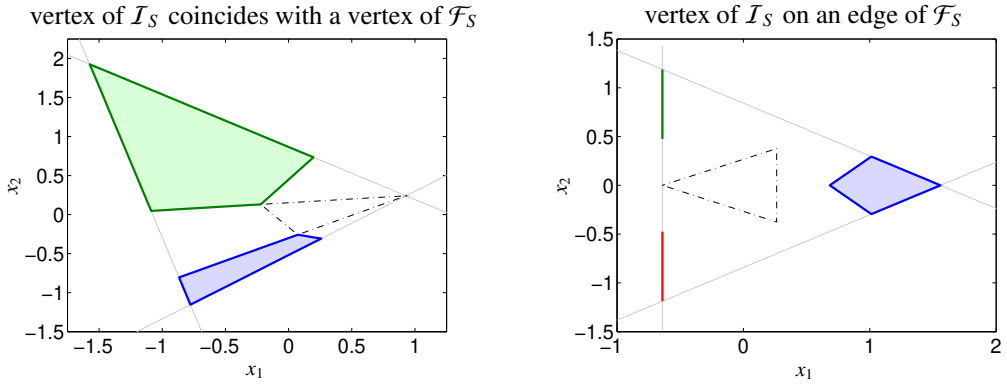

Figure 2: Left: A vertex of $\mathcal{I}_S$ coincides with a vertex of $\mathcal{F}_S$. This results in a unique spectrum or equivalently a one-point subset of the AFS $\mathcal{M}_S$. Right: A vertex of $\mathcal{I}_S$ is located on the boundary of $\mathcal{F}_S$ and not in a vertex of $\mathcal{F}_S$. Then the AFS $\mathcal{M}_S$ has two line-shaped subsets.

see also Eqs. (6) and (7) in [28]. With these polyhedra a simple geometric construction makes it possible to construct the AFS. For instance, the spectral AFS $\mathcal{M}_S$ is the set of all vertices of all $(s-1)$-simplices that include $\mathcal{I}_S$ and which are included in $\mathcal{F}_S$. An analogous property holds for AFS $\mathcal{M}_C$ and the polyhedra $\mathcal{I}_C$ and $\mathcal{F}_C$. In particular for $s = 3$ the 2-simplices are triangles which enclose INNPOL and are included in [17, 18]. A simultaneous construction of $\mathcal{M}_S$ and $\mathcal{M}_C$ is possible by using certain duality relations between $\mathcal{I}_C$ and $\mathcal{F}_S$ and also $\mathcal{I}_S$ and $\mathcal{F}_C$ [28, 30].

2.2. Data-based ambiguity reduction

The analysis in this section is inspired by the *selective regions* as introduced by Manne [6]. Such regions are subwindows with only one component. They can reduce the ambiguity considerably. Similarly important for our investigations is the paper of Rajkó et al. on data-based uniqueness [29]. In this work we derive a general result in the (somewhat technical) Theorem 2.1. Extreme cases of this theorem for special parameter settings are considered in Lemma 2.2 and reproduce a result of [29].

In order to give a gentle introduction, we consider the geometric situation that for a three-component system ($s = 3$) a vertex P of $\mathcal{I}_S$ is located on an edge of the polygon $\mathcal{F}_S$. If P is also a vertex of $\mathcal{F}_S$, then a unique spectrum is determined which is a direct outcome of the Borgen triangle rotation process. This is demonstrated in Figure 1 (left subplot). The Borgen triangle is drawn by dashed lines and cannot be rotated around INNPOL without intersecting INNPOL or FIRPOL. The bold dot marks a unique factor in the AFS plane. The centered subplot of Figure 1 shows that the point P cannot be moved in a continuous way to a close neighborhood of the first situation as otherwise the Borgen triangle intersects INNPOL. The situation is different if P hits a point on an edge of FIRPOL that is not a vertex of FIRPOL. The right subplot in Figure 1 shows two Borgen triangles (by dotted lines and by dashed lines) that indicate the existence of a line-shaped AFS subset.

The decisive point is that the existence of a zero element of the matrix D implies that a vertex of $\mathcal{I}_S$ is on the boundary of $\mathcal{F}_S$. The following theorem proves this. We illustrate this favorable situation again in Figure 2 by an AFS computation for $s = 3$. The left subplot of this figure shows a one-point AFS subset in the case that a vertex of $\mathcal{I}_S$ equals a vertex of $\mathcal{F}_S$ and the right plot shows two line-shaped subsets in the case that a vertex of $\mathcal{I}_S$ hits a boundary point of $\mathcal{F}_S$ that is not a vertex.

In the remaining part of the paper we always assume that the matrix D with the rank s has at least one factorization $D = CS^T$ with nonnegative factors of the rank s. We also assume that D^TD and DD^T are irreducible matrices, see Appendix A for the definitions. These assumptions should always be met for all non-degenerate problems. Otherwise, the AFS cannot be constructed, cf. [21].

Theorem 2.1. *Let $D \in \mathbb{R}^{k\times n}$ be a nonnegative matrix. For a number $s_0 \in \{1,\dots,s-1\}$ let $j_1,\dots,j_{s_0} \in \{1,\dots,n\}$ be indexes of s_0 spectral channels so that the spectral mixture data in the associated window has maximal rank*

$$\operatorname{rank}(D(:,[j_1,\dots,j_{s_0}])) = s_0. \tag{4}$$

Let $i_0 \in \{1,\dots,k\}$ be the index of a certain mixture spectrum so that the i_0th mixture spectrum does not contribute to the given frequency window. This means that

$$D(i_0,[j_1,\dots,j_{s_0}]) = (0,\dots,0) \in \mathbb{R}^{1\times s_0}. \tag{5}$$

Finally, let $\mathcal{S}$ be the intersection of the s_0 affine planes $\mathcal{P}_\ell$ with

$$\mathcal{P}_\ell = \{x \in \mathbb{R}^{s-1} :\ V(j_\ell, 2:s)x = -V(j_\ell,1)\}, \qquad \ell = 1,\dots,s_0. \tag{6}$$

Then it holds that:

1. *The set $\mathcal{S}$ is an $(s-1-s_0)$-dimensional surface element of the polyhedron $\mathcal{F}_S$. Depending on its dimension it is a vertex, an edge or a facet or an even higher dimensional surface element.*
2. *The vertex a_{i_0} of $\mathcal{I}_S$ is contained in $\mathcal{S}$.*
3. *$\mathcal{S}$ contains at least one feasible solution.*

In words, the theorem describes the following situation: Let a frequency window be given with the s_0 channel indexes $j_1,\dots,j_{s_0}$. Let the series of the mixture spectra restricted to these spectral channels have the full rank s_0 (this means that the underlying s_0 pure component spectra and the underlying s_0 pure component concentration profiles are linearly independent). If the i_0th mixture spectrum shows absorptions only outside this frequency window, then one vertex of $\mathcal{I}_S$ is located on a surface element of $\mathcal{F}_S$. Especially single zero entries in D or partially vanishing rows of D restrict parts of the spectral AFS to low-dimensional affine subspaces. [2] In particular, vanishing parts of rows of D are caused by isolated peaks and partially absent components.

Proof. For each $\ell = 1,\dots,s_0$ the vector a_{i_0} is contained in $\mathcal{P}_\ell$ since the condition in (6) is satisfied

$$V(j_\ell,2:s)a_{i_0} = a_{i_0}^T(V(j_\ell,2:s))^T = \frac{\left((U\Sigma)^T(2:s,i_0)\right)^T}{(U\Sigma)^T(1,i_0)}(V(j_\ell,2:s))^T = \frac{U\Sigma(i_0,2:s)}{U_{i_0}\sigma_1}(V(j_\ell,2:s))^T$$
$$= \frac{U(i_0,:)\Sigma(:,2:s)V^T(2:s,j_\ell)}{U_{i_0}\sigma_1} = \frac{\overbrace{D_{i_0,j_\ell}}^{=0 \text{ by } (5)} - U(i_0,:)\Sigma(:,1)V^T(1,j_\ell)}{U_{i_0}\sigma_1} = 0 - V^T(1,j_\ell) = -V_{j_\ell,1}.$$

Therefore a_{i_0} is an element of all affine hyperplanes $\mathcal{P}_\ell$ by (6). Since by (4)

$$s_0 = \operatorname{rank}(D(:,[j_1,\dots,j_{s_0}])) = \operatorname{rank}(U(\Sigma(:,1:s))(V([j_1,\dots,j_{s_0}],1:s))^T)$$

the last matrix factor must have full rank, i.e. $\operatorname{rank}(V(j_1,\dots,j_{s_0},1:s)^T) = s_0$. This proves the linear independence of its row vectors. Therefore the affine hyperplanes $\mathcal{P}_\ell$ (that are defined just by the row vectors of the latter matrix) do not show a linear dependence either. The intersection of the s_0 affine planes in the $(s-1)$-dimensional space is $(s-1-s_0)$-dimensional. Our general assumption on the existence of at least a single nonnegative factorization of D guarantees that $\mathcal{M}_S$ is not empty. Thus the simplex construction around $\mathcal{I}_S$ and in $\mathcal{F}_S$ is possible. Thus at least one point of $\mathcal{S}$, namely either a_{i_0} (cf. the situation in the left subplot of Fig. 1) or another points of $\mathcal{S}$ (cf. the situation in the right subplot of Fig. 1) represents a feasible solution. □

The special cases $s_0 = 1$ and $s_0 = s-1$ of Thm. 2.1 are summarized in explicit form in the following Result 2.2. For $s_0 = s-1$ a vertex of $\mathcal{F}_S$ coincides with a vertex of $\mathcal{I}_S$ and one isolated feasible solution is found; this result is not new, but has been described in [29] for three-component systems ($s = 3$).

Result 2.2. *Theorem 2.1 covers the following cases:*

[2] An affine space is a linear subspace that is shifted away from the origin by some translation vector.

1. *If $s_0 = 1$, then the rank condition* (4) *says that the j_1th column is not an all-zero vector and the zero-pattern-condition* (5) *shows that the j_1th column has a zero element in the i_0th row. Then the vertex a_{i_0} of $\mathcal{I}_S$ is located on the boundary of $\mathcal{F}_S$ since $V(j_1, 2:s)a_{i_0} = -V(j_1, 1)$. In other words, a single zero element of D implies that INNPOL touches FIRPOL.*

2. *If $s_0 = s - 1$, then the surface element $\mathcal{S}$ of $\mathcal{F}_S$ has the dimension $s - 1 - s_0 = 0$. A 0-dimensional surface element is a vertex of $\mathcal{F}_S$. Hence, a_{i_0} is an isolated feasible solution and its associated pure component spectrum is uniquely determined (except from scaling).*

An analogous form of Thm. 2.1 and Result 2.2 can also be derived for the concentrational AFS. This reads as follows:

Theorem 2.3. *On the given assumptions on $D \in \mathbb{R}^{k\times n}$ let a number $s_0 \in \{1, \ldots, s-1\}$ be given so that with the s_0 spectra indexes $i_1, \ldots, i_{s_0} \in \{1, \ldots, k\}$ the associated spectra submatrix attains its maximal rank*

$$\operatorname{rank}(D([i_1, \ldots, i_{s_0}], :)) = s_0.$$

Further let $j_0 \in \{1, \ldots, n\}$ be a certain frequency channel index so that D has the following zero pattern

$$D([i_1, \ldots, i_{s_0}], j_0) = (0, \ldots, 0)^T \in \mathbb{R}^{s_0}.$$

Finally let $\mathcal{S}$ be the intersection of the affine planes $\mathcal{Q}_\ell$ with

$$\mathcal{Q}_\ell = \{y \in \mathbb{R}^{s-1} : (U\Sigma)(i_\ell, 2:s)y = -(U\Sigma)(i_\ell, 1)\}, \qquad \ell = 1, \ldots, s_0.$$

Then it holds that:

1. *The set $\mathcal{S}$ is an $(s - 1 - s_0)$-dimensional surface element of the polyhedron $\mathcal{F}_C$. Depending on its dimension it is a vertex, an edge or a facet or an even higher dimensional surface element.*
2. *The vertex b_{j_0} of $\mathcal{I}_C$ is contained in $\mathcal{S}$.*
3. *$\mathcal{S}$ contains at least one feasible solution (a concentration profile).*

The proof entirely follows the lines of that of Thm. 2.1. The singular values have only a scaling effect. Alternatively, the result follows by applying Thm. 2.1 to the transposed matrix $D^T = SC^T$ as the factors C and S change their positions by the transposition.

The statement of Thm. 2.1 is illustrated by the following examples.

Example 2.4. 1. *We consider the consecutive reaction $X \to Y \to Z$ with concentration profiles and spectra as shown in Fig. 3. The spectra of Y and Z are single peaks with a different peak position and these two spectra are linearly independent in the upper frequency region. Hence Thm. 2.1 can be applied. Taking $s_0 = 2$ and j_{n-1}, j_n as frequency channel indexes, then $D(:, n-1:n)$ has the full rank 2 and $D(1, n-1:n) \approx (0, 0)$ so that the vertex a_1 of $\mathcal{I}_S$ equals one vertex of $\mathcal{F}_S$. So the associated pure component spectrum of X is uniquely determined, cf. Fig. 3.*

2. *Fig. 4 shows for reaction $X \to Y \rightleftharpoons Z$ another set of pure component concentration profiles and spectra.*

   The peak of the pure component spectrum of X is partially located outside the frequency windows of Y and Z. Further, the component X is absent in the final stage of the reaction. Then the conditions of Thm. 2.3 are fulfilled, e.g., for $i_0 = k$, $s_0 = 1$ $j_1 = 1$. So the vertex a_k of $\mathcal{I}_C$ is located on an edge of $\mathcal{F}_C$ since $\mathcal{S}$ is an $(s - 1 - s_0) = 1$-dimensional surface element of $\mathcal{F}_C$.

As a rule of thumb, many zero-entries of D (zero-columns or zero-rows are not acceptable however) result in a low rotational ambiguity. Then the AFS of a three-component system includes unique solutions (one-point subset) of a line-shaped AFS subset. The following example shows that this condition is not necessary in the sense that a matrix without any zero entries can have a unique factorization.

Example 2.5 (Compare to [32])**.** *Let*

$$C^T = S^T = \begin{pmatrix} 4 & 4 & 1 & 0 & 0 & 1 \\ 0 & 1 & 4 & 4 & 1 & 0 \\ 1 & 0 & 0 & 1 & 4 & 4 \end{pmatrix}.$$

The matrix $D = CS^T$ is strictly positive (with its smallest matrix entry equal to 1). No vertex of $\mathcal{I}_S$ is located on the boundary of $\mathcal{F}_S$. Nevertheless, D has the unique nonnegative factorization $D = CS^T$ (aside from permutations and scaling). Figure 5 shows $\mathcal{F}_S$, $\mathcal{I}_S$ and $\mathcal{M}_S$.

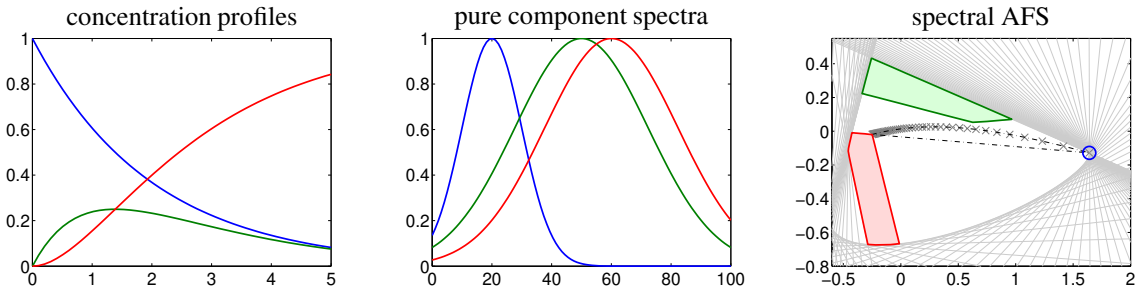

Figure 3: Analysis of first model problem presented in Example 2.4. The color code for the reaction $X \to Y \to Z$ is X (blue), Y (green) and Z (red). The green and the red components do not contribute to the first spectrum and both spectra show absorptions outside the frequency window of the blue component. Thm. 2.1 proves that one vertex of $\mathcal{I}_S$ (all vertices are marked by crosses $\times$ and are connected by a dash-dotted black line in order to form the boundary of INNPOL) coincides with one vertex of $\mathcal{F}_S$ (its boundary is drawn by gray lines). This results in the isolated feasible solution ($\circ$ in $\mathcal{M}_S$) and the blue spectrum is uniquely determined.

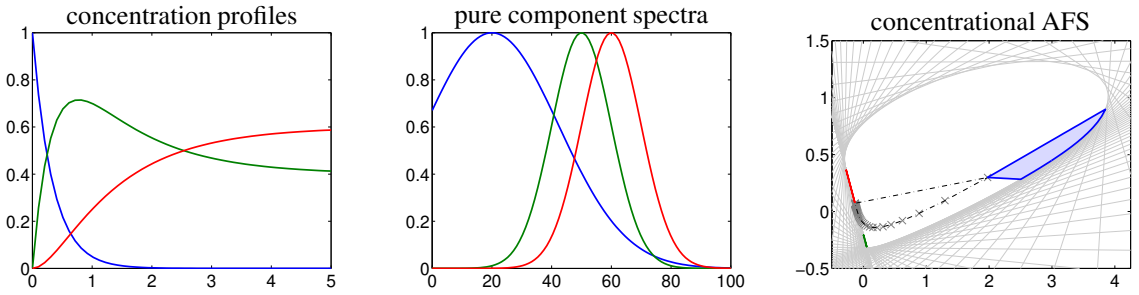

Figure 4: Analysis of the second model problem presented in Example 2.4. The color code for the reaction $X \to Y \to Z$ is X (blue), Y (green) and Z (red). Only the component X (blue) shows absorbance at small frequencies. In the second half of the time-interval the blue component is (nearly) absent, but the concentration profiles of Y and Z do not vanish there. The conditions of Thm. 2.1 are fulfilled with $s_0 = 1$, $i_0 = k$ and $j_1 = 1$. Hence (at least) one vertex of $\mathcal{I}_S$ (all vertices are marked by crosses $\times$ and are connected by a dash-dotted black line in order to form the boundary of INNPOL) is located on an edge of $\mathcal{F}_S$ (its boundary is drawn by gray lines). This results in an $(s - 1 - s_0) = 1$-dimensional surface element $\mathcal{S}$ of $\mathcal{M}$. The two line-shaped subsets of the AFS are located on $\mathcal{S}$.

2.3. Relevant and irrelevant spectra: Importance of proper concentration-combinations

The form and the size of the polyhedra INNPOL and FIRPOL determines the rotational ambiguity of the factorization problem - an obvious fact by the triangle/simplex rotation process of the Borgen plot construction. Hence let us discuss some geometric properties of these polyhedra. The numbers of facets of $\mathcal{F}_S$ and $\mathcal{F}_C$ as well as the numbers of vertices of $\mathcal{I}_S$ and $\mathcal{I}_C$ are limited by the dimensions k and n of D. Due to the duality relations [26, 33, 28] the number of facets of $\mathcal{F}_S$ equals the number of vertices of $\mathcal{I}_C$ and is smaller than or equal to n. Analogically, the number of facets of $\mathcal{F}_C$ equals the number of vertices of $\mathcal{I}_S$ and is smaller than or equal to k. Typically, the number k of spectra in D is higher than the number of vertices of $\mathcal{I}_S$ (as some the vectors a_i or b_i (3) are located in the interior of $\mathcal{I}_S$) and the number n of frequencies is higher than the number of vertices of $\mathcal{I}_C$ (as not each of the bounding half-spaces of the nonnegativity constraint must contribute to the boundary of $\mathcal{F}_S$).

Our goal is to design conditions for an experimental setup so that the rotational ambiguity of the associated nonnegative matrix factorization problem is as small as possible. Later in Def. 2.9 we introduce to this end the notion of *relevant* and *irrelevant* spectra/frequencies in D. Next, in a preparatory step, we analyze conditions under which a certain spectrum (a row of D) has a restrictive (volume decreasing) impact on $\mathcal{F}_C$ and an increasing (volume increasing) impact on $\mathcal{I}_S$. Analogically, we need to know whether a certain frequency (a column of D) has an impact on $\mathcal{F}_S$ and $\mathcal{I}_C$ or not. Theorem 2.6 and later Lemma 2.8 provide geometrically interpretable conditions (which, however, must be underpinned by a formal proof).

Theorem 2.6. *Let $D \in \mathbb{R}^{k\times n}$ be a nonnegative matrix satisfying our general assumptions, cf. the lines preceding Thm. 2.1. Let $i_0 \in \{1, \ldots, k\}$ be the index of a certain row of D (the i_0th measured spectrum).*

Then a_{i_0} by (3) *is a vertex of $\mathcal{I}_S$ if and only if no $\beta \in \mathbb{R}^k_+$ exists with*

$$D(i_0, :) = \sum_{\ell=1, \ell\neq i_0}^{k} \beta_\ell D(\ell, :). \tag{7}$$

(This means that the i_0th measured spectrum cannot be represented as a linear combination with nonnegative coefficients of the other spectra, namely the rows of D.)

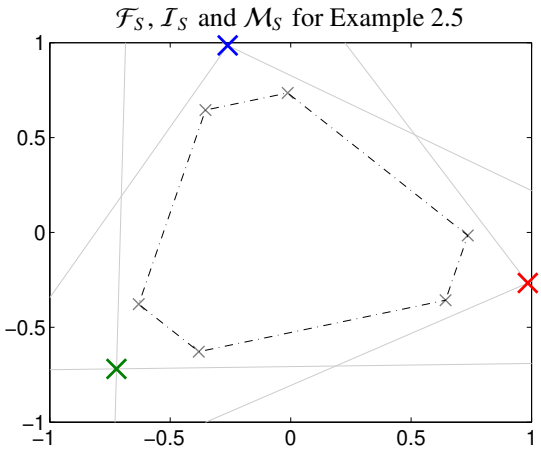

Figure 5: For the Example 2.5 the AFS $\mathcal{M}_S$ consists of the three isolated points drawn in blue, green and red. The polygon $\mathcal{I}_S$ of the 6×6 matrix D is plotted by the dash-dotted line. The boundary of $\mathcal{F}_S$ is limited by the gray lines that mark the bounding half-spaces according to the nonnegativity constraint. No vertex of $\mathcal{I}_S$ is on the boundary of $\mathcal{F}_S$. Nevertheless, a unique solution exists. Remark: Since $\sigma_2 = \sigma_3$ the SVD and the orientation of $\mathcal{M}_S$, $\mathcal{I}_S$ and $\mathcal{F}_S$ are not uniquely determined.

Proof. It is more convenient to prove the assertion in the following equivalent form: a_{i_0} is not a vertex of $\mathcal{I}_S$ if and only if a nonnegative vector $\beta \in \mathbb{R}^k$ exists so that (7) holds.

In order to prove this, we introduce the vectors

$$\widehat{a}_j = \begin{pmatrix} 1 \\ a_j \end{pmatrix} \in \mathbb{R}^s \quad \text{for } j = 1, \ldots, k.$$

By the definition of the convex polyhedron $\mathcal{I}_S$, a_{i_0} is not one of its vertices if it is a true convex combination of the a_ℓ with $\ell \neq i_0$. Equivalently, this condition holds for the extended vectors $\widehat{a}_j$. Thus a_{i_0} is not a vertex if a nonnegative vector $\alpha \in \mathbb{R}^k$ with at least two nonzero components exists with

$$\widehat{a}_{i_0} = \sum_{\ell=1,\ell\neq i_0}^{k} \alpha_\ell \widehat{a}_\ell, \qquad \sum_{\ell=1,\ell\neq i_0}^{k} \alpha_\ell = 1. \tag{8}$$

By (3) together with $D = U\Sigma V^T$ and $V^T V = I$ we get

$$a_i = \frac{(U\Sigma)^T(2:s,i)}{(U\Sigma)^T(1,i)} = \frac{(U\Sigma)^(i,2:s)}{(U\Sigma)(i,1)} = \frac{(U\Sigma V^T V)(i,2:s)}{(U\Sigma V^T V)(i,1)} = \frac{(DV)(i,2:s)}{(DV)(i,1)} = \frac{D(i,:)V(:,2:s)}{(DV)(i,1)}.$$

Thus the extended vectors $\widehat{a}_i$ can be written as

$$\widehat{a}_i = \frac{(U\Sigma)^T(:,i)}{(U\Sigma)^T(1,i)} = \frac{D(i,:)V}{(DV)(i,1)}.$$

We start the proof with inserting the $\widehat{a}_i$ in (8) which yields

$$\frac{D(i_0,:)V}{(DV)(i_0,1)} = \sum_{\ell=1,\ell\neq i_0}^{k} \alpha_\ell \frac{D(\ell,:)V}{(DV)(\ell,1)} \quad \text{and} \quad \sum_{\ell=1,\ell\neq i_0}^{k} \alpha_\ell = 1$$

or equivalently

$$\left[D(i_0,:) - \sum_{\ell=1,\ell\neq i_0}^{k} \alpha_\ell \frac{(DV)(i_0,1)}{(DV)(\ell,1)} D(\ell,:) \right] V = 0 \quad \text{and} \quad \sum_{\ell=1,\ell\neq i_0}^{k} \alpha_\ell = 1.$$

As the row spaces of D and V coincide, the orthogonality to V is equivalent to

$$D(i_0,:) - \sum_{\ell=1,\ell\neq i_0}^{k} \underbrace{\alpha_\ell \frac{(DV)(i_0,1)}{(DV)(\ell,1)}}_{\beta_\ell} D(\ell,:) = 0 \quad \text{and} \quad \sum_{\ell=1,\ell\neq i_0}^{k} \alpha_\ell = 1.$$

Thus the existence of a vector β with the components β_ℓ given above and further satisfying (7) has been shown. For completeness we still have to show that the β_ℓ are nonnegative. First, $\alpha_\ell \geq 0$. Second, the Perron-Frobenius condition on the first left singular vector, namely that $U(:,1) > 0$ or $U(:,1) < 0$, proves that

$$\frac{(DV)(i_0,1)}{(DV)(\ell,1)} = \frac{(U\Sigma V^T V)(i_0,1)}{(U\Sigma V^T V)(\ell,1)} = \frac{U(i_0,:)e_1\sigma_1}{U(\ell,:)e_1\sigma_1} = \frac{U(i_0,1)}{U(\ell,1)} > 0.$$

In order to complete the reverse direction of the assertion we finally have to show that β_ℓ rewritten as

$$\alpha_\ell = \beta_\ell \frac{(DV)(\ell,1)}{(DV)(i_0,1)}$$

satisfies the equation $\sum_{\ell=1,\ell\neq i_0}^{k} \alpha_\ell = 1$. This is proved by

$$\sum_{\ell=1,\ell\neq i_0}^{k} \alpha_\ell = \frac{1}{(DV)(i_0,1)} \underbrace{\left(\sum_{\ell=1,\ell\neq i_0}^{k} \beta_\ell (DV)(\ell,1) \right)}_{=D(i_0,:) \text{ by (7)}} V(:,1) = \frac{D(i_0,:)V(:,1)}{(DV)(i_0,1)} = 1.$$

□

Thm. 2.6 can be interpreted as follows: A mixture spectrum, namely a row of D, enlarges $\mathcal{I}_S$ and thus restricts $\mathcal{M}_S$ if and only if it is not a linear combination with nonnegative coefficients of the remaining spectra in D. The relation to the (original pure component) factor C is treated in the following Lemma 2.7. Simultaneously, $\mathcal{M}_C$ is decreased due to a decreasing size of $\mathcal{F}_C$.

Lemma 2.7. *On the assumptions of Thm. 2.6 let CS^T be a nonnegative matrix factorization of D.*

The i_0th measured spectrum $D(i_0,:)$ is a linear combination with nonnegative coefficients of the remaining spectra (rows of D) if and only if $C(i_0,:)$ is a linear combination with nonnegative coefficients of the remaining rows of C.

Proof. It holds for the nonnegative vector $\beta \in \mathbb{R}^k$

$$D(i_0,:) = \sum_{\ell=1,\ell\neq i_0}^{k} \beta_\ell D(\ell,:) \quad \Leftrightarrow \quad \left(C(i_0,:) - \sum_{\ell=1,\ell\neq i_0}^{k} \beta_\ell C(\ell,:) \right) S^T = 0 \quad \Leftrightarrow \quad C(i_0,:) = \sum_{\ell=1,\ell\neq i_0}^{k} \beta_\ell C(\ell,:).$$

The last equivalence holds since $S \in \mathbb{R}_+^{n\times s}$ has the rank s so that a linear combination of the columns of D is the null vector if and only if all expansion coefficients are zero. □

A numerical test of the linear combination conditions of Thm. 2.6 and Lemma 2.7 in the form of an *a posteriori* analysis requires a practically executable test. For a proper tolerance parameter ε it has to be tested for each i_0 whether or not a nonnegative β exists such that the condition

$$\left\| C(i_0,:) - \sum_{\ell=1,\ell\neq i_0}^{k} \beta_\ell C(\ell,:) \right\|_2^2 < \varepsilon$$

is fulfilled. The tolerance parameter ε must be sufficiently small. For example in the (usual) model problem from Example 2.4, cf. Fig. 4, a number of 22 indexes i_0 of the $k = 50$ rows of C result in a residuum smaller than $\varepsilon = 10^{-10}$. However, for the model data each $D(i_0,:)$ has an impact on $\mathcal{I}_S$. This shows that this criterion is difficult to evaluate even for model data. Furthermore, preprocessed spectral data can contain negative data elements close to zero and also comparable small negative matrix elements of C and S should sometimes be accepted. In order to overcome these problems we present in Sec. 2.4 a possible and stable strategy to deal with such data.

The combination of Lemma 2.7 with Thm. 2.6 yields the result that a spectrum $D(i_0,:)$ enlarges $\mathcal{I}_S$ and restricts $\mathcal{F}_C$ if and only if the associated (true) concentration $C(i_0,:)$ is not a linear combination of the remaining concentration profiles. Analogically, Thm. 2.6 can be reformulated for the spectral factor.

Lemma 2.8. *Let the assumptions of Thm. 2.6 be fulfilled. Then b_{i_0} is a (true) vertex of $\mathcal{I}_C$ and its dual affine hyperplane is a (true) facet of $\mathcal{F}_S$ if and only if there is no nonnegative vector $\beta \in \mathbb{R}^k$ with*

$$D(:,i_0) = \sum_{\ell=1,\ell\neq i_0}^{n} \beta_\ell D(:,\ell).$$

All these results allow us to make a distinction between relevant and irrelevant spectra/frequencies as follows:

Definition 2.9. *Let D have non-empty AFS-sets $\mathcal{M}_C$ and $\mathcal{M}_S$ of feasible solutions. A mixed spectrum $D(i_0, :)$ is called relevant if it has an impact on $\mathcal{F}_C$ (and thus also on $\mathcal{I}_S$) and irrelevant otherwise. Let k^* be the number of all relevant spectra of D.*

In an analogous way a frequency is called relevant if $D(:, j_0)$ has an impact on $\mathcal{F}_S$ (and thus also on the dual polyhedron $\mathcal{I}_C$) and irrelevant otherwise. Let n^* be the number of all relevant frequencies of D.

The notion of relevant and irrelevant spectra/frequencies is related to the popular window factor analysis (WFA, [34]) and also to the evolving factor analysis (EFA, [35]). WFA is applied to analyze subwindows along the frequency indexes of D. Typically only some of the chemical components show an absorption in these windows which makes a subsystem analysis possible. Since only extremal absorptivity-relations restrict $\mathcal{F}_S$, we conclude that only few components contribute to the relevant frequency channels. Figs. 10 and 11 (which will be introduced later) illustrate that these regions (of relevant frequency channels) are related to proper frequency subwindows of a WFA.

Similarly, EFA supports the analysis in the time direction, namely if certain components arise or participate to the reaction. Since only extremal concentration-relations expand $\mathcal{I}_S$, we conclude that only few components contribute to the relevant spectra. This is also demonstrated in Fig. 12.

2.4. A posteriori analysis in terms of relevant and irrelevant frequencies/spectra for model and perturbed data

Theorem 2.6 allows us to subdivide the index set $\{1, \ldots, k\}$ into sets of relevant and irrelevant spectra for the idealized case of model data. Analogically, Lemma 2.8 enables a similar distinction for relevant and irrelevant frequency channels. Next we demonstrate how these distinctions can be made for perturbed or noisy data.

The starting point is the polyhedron $\mathcal{F}_S$. Then D is changed in the way that single columns are removed, which means that single frequency channels are dropped from the series of spectra. If the ℓth column is removed, then the column-dropped matrix is

$$\widetilde{D}^{(\ell)} = D(:, [1 : \ell - 1, \ell + 1 : n]) \in \mathbb{R}^{k \times n-1} \qquad \text{for} \quad \ell = 1, \ldots, n.$$

Then we compute the associated polyhedron FIRPOL, denoted by $\widetilde{\mathcal{F}}_S^{(\ell)}$, for $\widetilde{D}^{(\ell)}$. For this computation the right singular vectors of D are used (of course $V(\ell, :)$ is removed). The channel that belongs to the index ℓ is said to be *relevant* if $\widetilde{\mathcal{F}}_S^{(\ell)}$ differs from $\mathcal{F}_S$. To this end the two approximating polygons are first compared with respect to their numbers of vertices and in the case of the same number of vertices with respect to the positions of the vertices.

A similar procedure is applied to the rows of D. The removal of the νth mixture spectrum results in the row-dropped matrix

$$\widehat{D}^{(\nu)} = D([1 : \nu - 1, \nu + 1 : k], :) \in \mathbb{R}^{k-1 \times n} \qquad \text{for} \quad \nu = 1, \ldots, k.$$

In this case, FIRPOL $\widehat{\mathcal{F}}_C^{(\nu)}$ is computed for the concentration factor. The resulting polyhedron is compared with the reference solution $\mathcal{F}_C$. For $s = 3$ the polyhedra are (planar) polygons and are computed by the polygon inflation procedure [20, 21, 30]. Hence the computations are stable even for noisy data.

2.5. Matrix augmentation

It is commonly believed that the combination of multiple spectral measurements in the form of a *matrix augmentation* is a proper way in order to reduce the rotational ambiguity. Often a combination of two data sets for the same chemical reaction system (with the same pure component spectra but with modified concentration profiles, which might result from changed reaction conditions) shows an ambiguity reduction only for one of the data sets. The following example illustrates a case in which each of the data sets profit in a reduction of the ambiguity by matrix augmentation.

Example 2.10. *We consider the consecutive model reaction $X \xrightarrow{k_1} Y \xrightarrow{k_2} Z$ with the reaction rate constants k_1 and k_2. Two sets of reaction rate constants are used, namely $K^{(1)} = (k_1^{(1)}, k_2^{(1)}) = (1, 0.5)$ and $K^{(2)} = (k_1^{(2)}, k_2^{(2)}) = (1, 4)$. The associated concentration profiles are computed for the time interval $t \in [0, 5]$ with $k = 50$ equidistant grid points. The concentration profiles as well as the pure component spectra of X, Y and Z are plotted in the first row of Fig. 6. Let $D^{(1)}$ be the spectral data matrix for the reaction rate constants $K^{(1)}$ and let $D^{(2)}$ be the matrix $K^{(2)}$. Furthermore, let $D^{(3)} = [D^{(1)}, D^{(2)}]$ be the augmented spectral data matrix that combines the first two data sets.*

Next the spectral AFS sets for $D^{(i)}$, $i = 1, 2, 3$, are computed. As the singular vector column spaces of the augmented matrix $D^{(3)}$ contain the corresponding spaces of $D^{(1)}$ and $D^{(2)}$ all results are transformed to the joint singular vector bases of $D^{(3)}$. This provides the basis for a comparison of the AFS sets that are plotted in the second row of

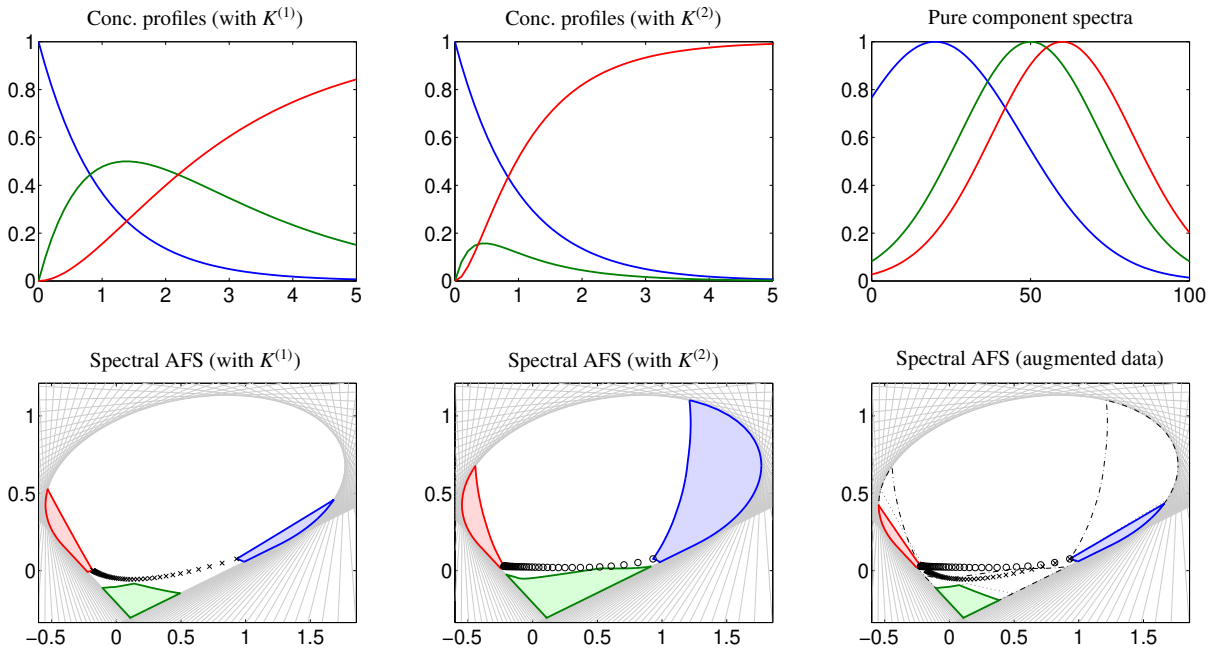

Figure 6: Matrix augmentation and the reduction of rotational ambiguity as explained in Example 2.10. Upper row: The two sets of concentration profiles and the joint pure component spectra. Lower row: The three spectral AFS sets. The vectors a_i by (3) are plotted by $\times$ symbols for $D^{(1)}$ and by $\circ$ symbols for $D^{(2)}$. The spectral AFS-sets of $D^{(1)}$ (dotted lines) and of $D^{(2)}$ (dash-dotted lines) are added to the spectral AFS for $D^{(3)}$. Therein the complementing effect of the a_i for different settings is obvious. Both spectral data matrices contribute with relevant spectra to the augmented data. All AFS-sets are presented with respect to the joint SVD basis of the augmented matrix $D^{(3)}$ in order to make a direct comparison possible.

Fig. 6. A reduction of the rotational ambiguity can be stated especially from $D^{(2)}$ to $D^{(3)}$. The effect is caused by different combinations of concentrations as described in Lemma 2.7 and Thm. 2.6. The set $\mathcal{F}_S$ is the same for $i = 1, 2, 3$ as the right singular vectors must always be the same since the pure component spectra are not changed. Further, $\mathcal{I}_S$ for $i = 3$ is the convex closure of the union of the sets $\mathcal{I}_S$ for $i = 1$ and $i = 2$. Hence the AFS for the augmented data $D^{(3)}$ must be the smallest one. The spectra of $D^{(1)}$ together with the last spectrum of $D^{(2)}$ contribute exclusive restrictions due to extremal concentration relations. According to Definition 2.9 each of the matrices $D^{(i)}$, $i = 1, 2$, provides relevant spectra for the augmented data.

If a much wider time interval $[0, 15]$ is used, then we observe that $\mathcal{I}_S$ for $i = 2$ is contained in $\mathcal{I}_S$ for $i = 1$. As $\mathcal{F}_S$ is unchanged the first case cannot profit from data augmentation by the second system. However, the matrix of $D^{(2)}$ by $D^{(1)}$ has a restrictive effect since $\mathcal{I}_S$ of the augmented matrix is that of $D^{(1)}$. The reason for this is that the product component Z at $t = 15$ also solely occurs for $i = 1$ since $C^{(1)}(k, :) \approx (3 \cdot 10^{-7}, 1 \cdot 10^{-3}, 1)$.

3. How to reduce the rotational ambiguity by designing the chemical experiment

As shown so far, the size and the form of the polyhedra INNPOL and FIRPOL determine the extent of the rotational ambiguity. The crucial question is how a chemical experiment should be designed so that the rotational ambiguity underlying its associated pure component factorization problem is as small as possible. In the following we summarize some general conditions to achieve this goal. We distinguish the frequency axis and the time axis. First, the conditions along the frequency axis concern properties of the pure component spectra. Typically, the chemical components of the reaction are fixed and hence the pure component spectra cannot be changed. However, changing the spectral method (e.g. from UV/Vis to IR or Raman) may result in other spectral properties. Second, the conditions along the time axis concern the form of the concentration profiles. The concentration profiles can be varied by changes of the experimental conditions (reaction time, temperature, pressure, solvent etc.).

Recommendations 1 (Frequency axis/Properties of the pure component spectra)**.** *The following conditions should be fulfilled in order to support a small rotational ambiguity:*

1. *Isolated peaks or spectral intervals containing only few absorbing chemical components are preferred, see Thm. 2.1.*
2. *By selecting proper frequency intervals spectral contributions of non-interesting chemical components (e.g. from the solvent) should be excluded. Otherwise the number s of chemical components increases together with the complexity of the pure component factorization problem and the extent of the rotational ambiguity.*

3. *If some of the pure component spectra contribute to separated frequency windows, then try to analyze the subsystems step-by-step.*
4. *If a certain pure component spectrum $a \in \mathbb{R}^n$ is known and for some reason equality constraints cannot be applied, then extend D as*

$$\widetilde{D} = \begin{pmatrix} D \\ \gamma a^T \end{pmatrix} \in \mathbb{R}^{(k+1)\times n}. \tag{9}$$

Therein, the scaling parameter γ is important for limiting the impact of noise and perturbations on a. A useful choice is $\gamma = 0.1 \max(D)/\max(a)$. Thm. 2.6 applies to this situation since $C(k+1,:)$ with the chemically correct factor C has exactly one non-zero entry.

Recommendations 2 (Time axis/Properties of the pure component concentration profiles)**.** *The following conditions should be fulfilled in order to support a small rotational ambiguity:*

1. *Localized concentration profiles, i.e. not all chemical components are always present, are preferred, see Thm. 2.3.*
2. *Spectra are to be measured over a long time since for finished chemical (non-equilibrium) reactions the first point should be fulfilled.*
3. *If a certain concentration profile $c \in \mathbb{R}^k$ is known and if equality constraints cannot be used, then extend D as*

$$\widetilde{D} = (D,\ \gamma c) \in \mathbb{R}^{k\times(n+1)}. \tag{10}$$

Therein the scaling parameter γ is important for limiting the impact of noise and perturbations on c. A useful choice is $\gamma = 0.1 \max(D)/\max(c)$. Lemma 2.8 applies to this situation, since $S(n+1,:)$ with the chemically correct factor S has exactly one non-zero entry.

Let us remark that the influence of additionally taken mixture spectra or additionally taken spectral channels (e.g. by using another frequency range by a different spectral method) is as follows:

- An additionally measured mixed spectrum reduces $\mathcal{F}_C$ and enlarges $\mathcal{I}_S$ if and only if the underlying concentration profile is not a nonnegative linear combination of the previous concentration profiles. See Thm. 2.6 and Lemma 2.7.
- An additionally taken spectral channel reduces $\mathcal{F}_S$ and enlarges $\mathcal{I}_C$ if and only if the underlying spectrum is not a nonnegative linear combination of the previous spectra. See Thm. 2.6 and Lemma 2.8.

4. Intrinsic or base level rotational ambiguity

Realistically, one cannot expect that changes of the reaction conditions of a fixed chemical reaction can transform the mixture data matrix D in a way that a unique pure component decomposition can be determined. Possible changes of the reaction conditions concern the pressure, the temperature or the solvent. Moreover, further mixture spectra can be added to the spectral data matrix D and also new frequency ranges can be used for the spectral measurements. However, one typically observes a non-reducible remaining base level of rotational ambiguity. This base level of ambiguity depends on the pure component spectra that cannot be changed without changing the reaction system. For instance, if the pure component spectra are highly overlapping, then even completely separated concentration profiles (aside from the fact that the mass balance would not allow such profiles) would not result in mixture data with a unique pure component factorization. Instead, one observes that such systems show some intrinsic rotational ambiguity whose minimal extent is determined by the degree of overlap of the pure component spectra. The intrinsic base level of ambiguity can be made accessible by combinations of concentration profiles which show some extremal behavior.

A challenge for future research is a systematic analysis of this intrinsic base level ambiguity. Once again, the key for an understanding of these relations is the geometric point of view. The point is that $\mathcal{F}_S$ is completely determined by the pure component spectra. Further, any increase of $\mathcal{I}_S$ can decrease $\mathcal{M}_S$. There is an extremal (largest) simplex INNPOL, which contains all the data representatives a_i for all possible linear combinations of the concentration profiles. This largest polygon $\mathcal{I}_S$ determines the smallest AFS $\mathcal{M}_S$, namely the base level ambiguity.

5. Application to experimental spectral data

Three non-model data sets from catalytic reaction systems are taken for a demonstration and discussion of the results achieved so far. Reductions of the rotational ambiguity are proved. We do not claim to present an ultimate answer by means of our a posteriori analysis. Instead, we intend to foster a future discussion of DoE principles on the ambiguity reduction in MCR factorizations. Our discussion is based on the following FT-IR and UV/Vis spectral data sets. For some of these reaction systems we assume a kinetic model, but there is no necessity to presuppose the

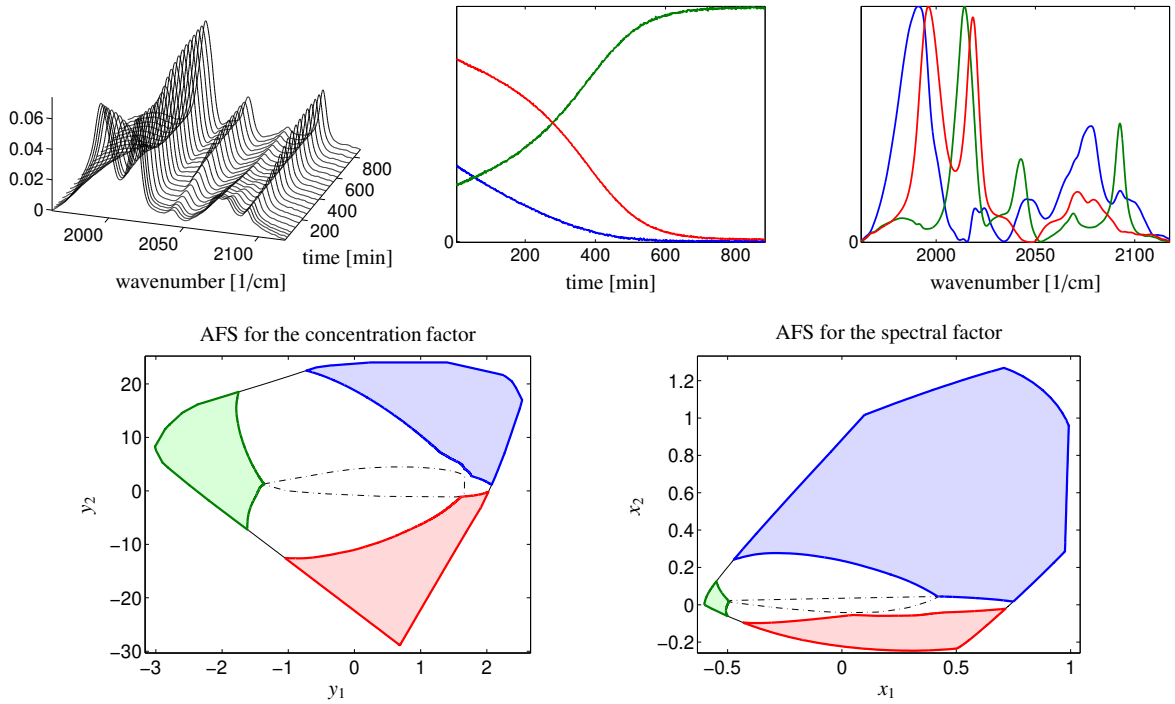

Figure 7: Data set 1: The mixture spectra are plotted in the upper row (left). Only every 40th spectrum is shown. The non-scaled kinetic hard-model based decomposition is plotted in the same row. The AFS-sets $\mathcal{M}_S$ and $\mathcal{M}_C$ are computed by the polygon inflation algorithm and are shown in the lower row. The generalized polygons FIRPOL (solid black line) and INNPOL (dash-dotted black line) are also plotted in the AFS, see [30] for their computation.

availability of such a model in general. However, in the context of our analysis it is often convenient to assume a kinetic model in order to demonstrate that the ambiguity reducing techniques do not overshoot the mark in the sense that the true solution is finally excluded.

Data set 1. *The FT-IR data set concerns a subsystem of the rhodium-catalyzed hydroformylation process, namely the process of the catalyst formation, see [36]. The data set contains* $k = 850$ *spectra taken in the time interval* $[4.72, 883.61]$min*. A number of* $n = 645$ *frequency channels is used in the wavenumber interval* $[1962.3, 2117.6]\text{cm}^{-1}$*. After a background-subtraction only three chemical components show a main contribution to these spectra, namely the olefin, the hydrido complex and the acyl complex. Fig. 7 shows the series of mixture spectra, the pure component spectra and the associated concentration profiles (as gained by an MCR analysis that includes a kinetic hard model) and the two AFS-sets for the concentration factor and the spectral factor.*

Data set 2. *The UV/Vis spectra of this data set are taken from [37, 38]. The reaction is on the formation of linear α-olefines from ethylene with a hafnium complex as catalyst. A number of* $n = 381$ *spectral channels is taken in the wavelength interval* $[420.3, 800.3]$nm*. The first non-reliable spectrum has been removed from the data set so that* $k = 499$ *spectra remain in the time interval* $[0.005, 2.49]$s*. The singular values reveal* $s = 3$ *major absorbing components. See Fig. 8 for the series of mixture spectra, the hard-model based solution (using the underlying kinetic model* $X \rightarrow Y \rightarrow Z$*) and the AFS-sets for the pure component spectra and concentration profiles.*

Data set 3. *The series of FT-IR spectra is on the formation of Rh(0) carbonyls resulting from an "unwanted´´ side reaction during the generation of a catalytically active rhodium hydrido carbonyl complex from* $Rh(acac)(CO)_2$*. The experiment was run at* 303K *and* 20bar *synthesis gas pressure (*$CO{:}H_2$*=1:1). The initial concentration of* $Rh(acac)(CO)_2$ *was* $6.6 \cdot 10^{-4}$mol/L *in the solvent cyclohexane. The major absorbances are from the "unwanted" rhodium carbonyl clusters* $Rh_4(CO)_{12}$ *and* $Rh_6(CO)_{16}$ *as well as from the* $Rh(acac)(CO)_2$*. By a background subtraction the spectrum of cyclohexane has been mostly removed. The number of spectra is* $k = 290$*, each spectrum contains* $n = 2739$ *spectral channels. See [39] for a complete chemometric analysis of this data set. Fig. 9 shows the mixture spectra, the extracted "true" pure component decomposition and the associated AFS-sets.*

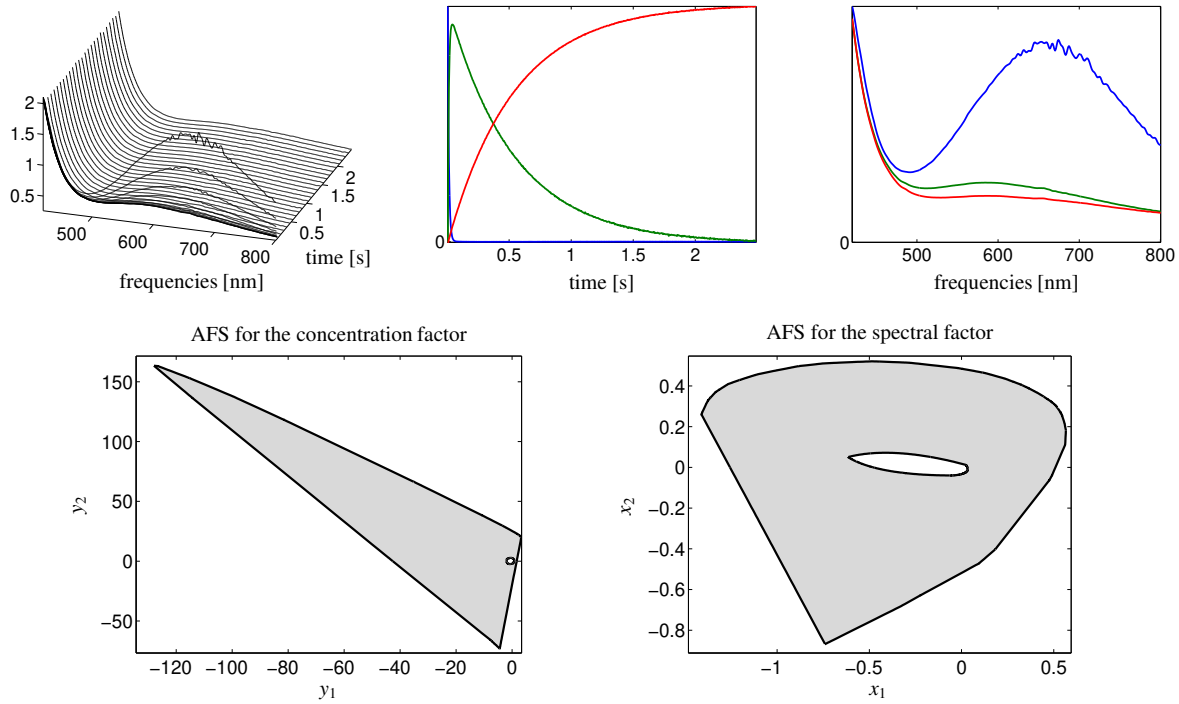

Figure 8: Data set 2: The mixture spectra are plotted in the upper row (left). The first 10 spectra are completely plotted and then only every 20th spectrum. The non-scaled kinetic hard-model based decomposition is also shown in the upper row. The AFS-sets $\mathcal{M}_S$ and $\mathcal{M}_C$ are plotted in the lower row.

5.1. Analysis of data-based ambiguity criteria

Next we discuss the restrictive effect of isolated peaks or partially non-absorbing components (cf. Sec. 2.2) for the three data sets. As the experimental spectral data contains noise and perturbations, the classical Borgen plots must be substituted by dual Borgen plots or polygon inflation. Thus the uniqueness criteria are softened and hold in an approximate sense.

Data set 1: Thm. 2.1 can only be applied in an approximate way (with $s_0 = 2$). Fig. 7 indicates that the green component shows relatively small absorptions in the wavenumber interval [1962, 2000]cm^{-1} whereas the two other components show strong linearly independent absorbtions. Hence the rank condition (4) is fulfilled. Since in the final stage of the reaction only the green component is present (thus (5) is approximately satisfied), the green subset of the spectral AFS is relatively small. Unfortunately the noise level in the data is so large that none of the blue or red subsets of the *concentrational* AFS are degenerated to line-shaped or thin-band shaped subsets of the AFS. However, for model-data or data with a low noise level the duality theory predicts that a point-shaped AFS subset is dual to the line-shaped AFS subset of the dual factor.

Data set 2: Since all pure component spectra have significant absorptions in the complete frequency interval, no isolated or small AFS subsets exist. And in fact, the two AFS-sets are topologically connected sets each including a hole around the origin. Such a behavior is typically observed for the UV/Vis spectroscopy with its broad peaks.

Data set 3: Each of the three pure component spectra has nearly isolated peaks. This can be expected by inspecting the series of mixture spectra. At the beginning of the reaction only the blue component is present. Hence we can apply Thm. 2.1 with $s_0 = 2$. This results in an isolated solution; due to noise we get a small blue subset in the spectral AFS. Furthermore, since the blue component is nearly absent in the second half of the reaction, we can apply Thm. 2.1 a second time with $s_0 = 1$. Due to the isolated peak in the blue pure component spectrum this leads to the situation where several points a_i, $i \geq 175$ are very close to the boundary of $\mathcal{F}_S$. Consequently the green and the red subset of the spectral AFS must be narrow stripes.

5.2. A posteriori redundancy-analysis of the spectral data

The spectral data matrix D usually contains a lot of redundant information. Only few of its rows and columns determine the geometric structure of the polyhedra INNPOL and FIRPOL and the resulting AFS. In order to distinguish relevant (i.e. structure determining parts of the series of spectra) and irrelevant (i.e. redundant information) rows and columns of D we have introduced in Sec. 2.3 the notion of relevant and irrelevant rows and columns. Next we apply this redundancy analysis to our three experimental spectral data sets. The irrelevant spectral channels and the

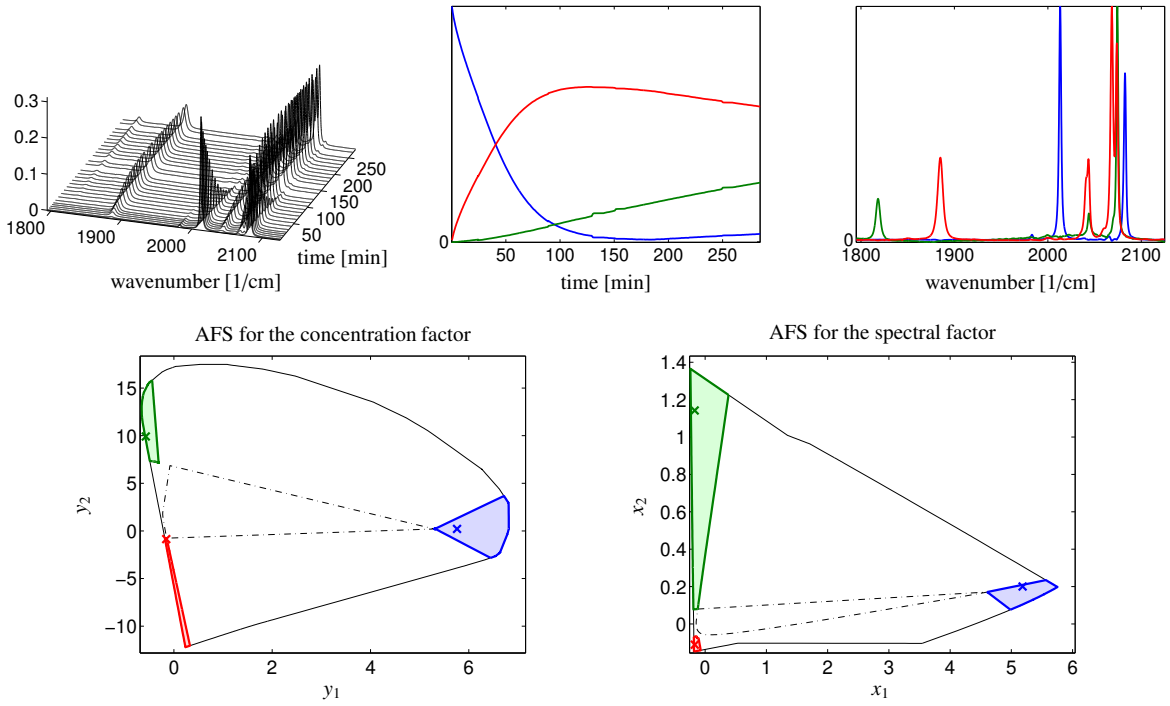

Figure 9: Data set 3: The mixture spectra are plotted in the upper row (left). Only every 10th spectrum is shown. The non-scaled kinetic hard-model based decomposition is also shown in the upper row. The AFS-sets $\mathcal{M}_S$ and $\mathcal{M}_C$ are plotted in the lower row. (bottom). The boundary of the generalized polygon FIRPOL is drawn by a solid black line and the boundary of INNPOL by a dash-dotted black line.

irrelevant spectra have no impact on the AFS-sets. We start with the analysis of the data set 3 since all effects can be explained for this data set in the best way.

We get the surprising result that only few parts of the spectral mixture data are responsible for the ambiguity of the pure component factors; the results are illustrated by the three figures 10–12. In these figures the color cyan is used to mark the relevant, non-redundant parts of the mixture spectra and the pure component profiles. The results can potentially be used in order to reduce the spectral observation only to some decisive spectral regions and to some time intervals. Practically, this can be exploited in the case of a repeated and refined spectral investigation of the chemical reaction system. These results essentially reproduce Manne's theorems, however for the case of noisy data and with respect to an AFS representation of the ambiguity.

Data set 3: The polygons $\mathcal{F}_C$ and $\mathcal{F}_S$ are computed by the polygon inflation method [20, 21, 30]. The control parameters for these computations are $\varepsilon = 0.015$ (acceptance level on small negative entries in C and S), $\varepsilon_b = 10^{-7}$ (boundary precision) and $\delta = 10^{-6}$ (stopping criteria). See [20, 21, 30] for details on these control parameters. In [30] the two parameters $\varepsilon_C, \varepsilon_S$ are used instead of the single parameter ε. For the data set 3 the a posteriori analysis leads to small numbers of $n^* = 25$ relevant frequency channels and $k^* = 73$ relevant spectra. All other frequency channels can be considered to be redundant. The reduced matrix $\widehat{D} \in \mathbb{R}^{73\times 25}$ which is formed from the relevant frequency channels and the relevant spectra has the same AFS-sets as the full non-reduced matrix $D \in \mathbb{R}^{290\times 2739}$. The relevant frequency channels are marked by the color cyan in the left and the centered subplots of Fig. 10. An interesting observation is that all the relevant frequency channels are at peak centers or close to the peak centers. All the other frequency channels do not determine the structure of INNPOL and FIRPOL - they contain only redundant information. In the right plot of Fig. 10 the relevant points along the time axis (or equivalently the relevant mixture spectra) are marked along the time axis by vertical lines in cyan. The ratio k^*/k of relevant mixture spectra is significantly higher than the ratio n^*/n of relevant frequency channels. In other words, many of the mixture spectra contribute to the boundary of the representing polygon.

Data sets 1 and 2: The results of the analogous redundancy analysis for the data set 1 with $\varepsilon = 7 \cdot 10^{-3}$ results in a number of $n^* = 118$ relevant frequency channels and a number of $k^* = 38$ relevant spectra. The graphical representation is shown in Fig. 11. For data set 2 and with $\varepsilon = 2.5 \cdot 10^{-3}$ the number of relevant frequencies is $n^* = 71$ and the number of relevant spectra is $k^* = 25$. The results are plotted in Fig. 12.

5.3. Lower bounds on the rotational ambiguity for data set 1

Next the lower bounds on the rotational ambiguity as explained in Sec. 4 are explicitly determined for the data set 1. As we do not intend to change the chemical reaction (the pure component spectra are fixed but we allow changes

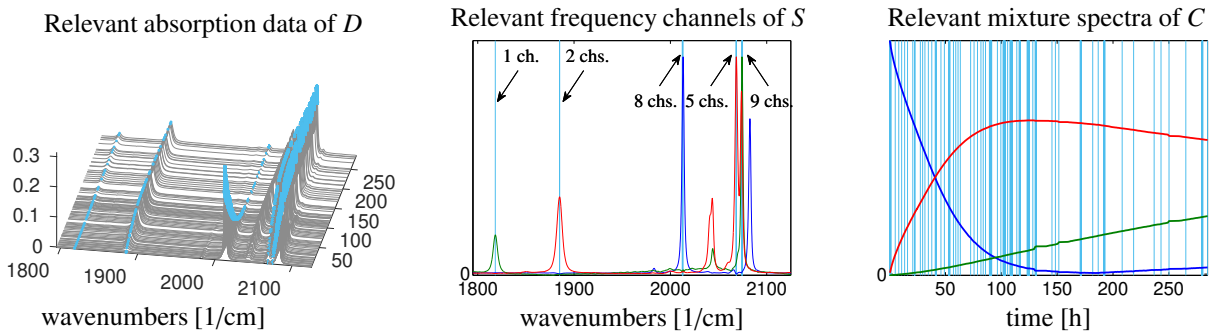

Figure 10: A posteriori redundancy analysis for the data set 3. Left: Relevant parts of the mixture spectra are marked by the color cyan. Center: Vertical lines mark the $n^* = 25$ frequency channels that determine the shape of $\mathcal{F}_S$ and $\mathcal{I}_C$. Right: Cyan vertical lines mark the $k^* = 73$ points in time (times of measurement of the mixture spectra) that have an impact on the sets $\mathcal{F}_C$ and $\mathcal{I}_S$.

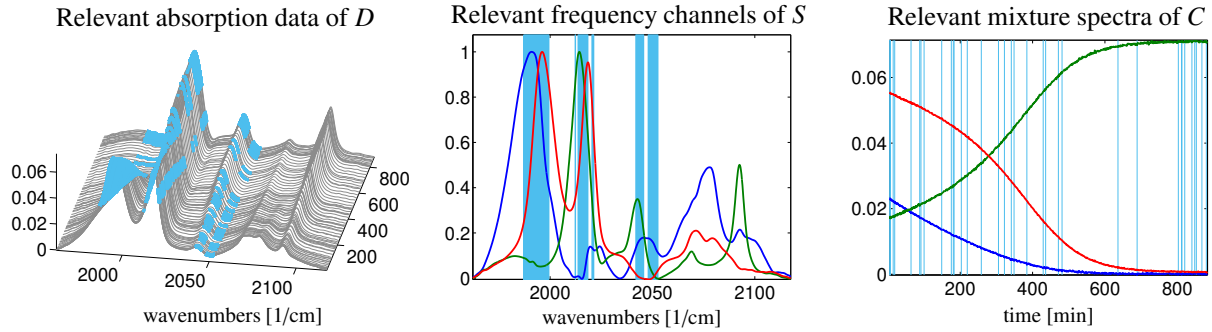

Figure 11: A posteriori redundancy analysis for the data set 1. Only $n^* = 118$ frequency channels (cyan lines/areas) that have an impact on the polygons $\mathcal{F}_S$ and $\mathcal{I}_C$. Further, only $k^* = 38$ mixture spectra (the times of their measurements are marked by vertical lines in cyan) have an impact on the polygons $\mathcal{F}_C$ and $\mathcal{I}_S$. The control parameter on the acceptance of small negative entries of C and S is $\varepsilon = 7 \cdot 10^{-3}$. In the left plot only every 8th irrelevant spectrum is plotted (black lines) but all relevant spectra (cyan lines) are plotted.

of the reaction conditions and of the spectral measurements) a certain base level of ambiguity must be accepted. The lower bounds on the ambiguity are computed in an a posteriori process. To this end we augment the spectral data matrix D by the pure component spectra. Then the true, chemically correct factorization of the augmented matrix includes the associated extremal concentration values in terms of a diagonal submatrix.

The data augmentation for data set 1 is done in a way similar to (9) by adding the pure component spectra of the olefin (blue) and acyl complex (red) in a joint, single step. The parameter γ is taken as $\gamma = 0.01 \max(D)/\max(a)$. Hence $\widetilde{D} \in \mathbb{R}^{852\times 645}$. There is no need to add the pure component spectrum of the hydrido complex as well, since this complex is solely present in the final stage of the reaction. The resulting lower bounds of the AFS subsets are presented in Fig. 13. Obviously a certain level of rotational ambiguity must be stated. As this experimental spectral data set contains noise, not all of the representatives of the pure component spectra are located on the boundary of $\mathcal{I}_S$. (This would be the case of noise-free model data.) For this augmented spectral data set the number of relevant spectra is $k^* = 15$ instead of $k^* = 38$ for the original spectral data. In particular the augmented pure component spectra belong to the relevant ones. The resulting message is that even an optimal design of the experiments cannot force a unique decomposition for this system.

5.4. Augmentation of the spectral data matrix by a concentration profile for data set 2

Finally, we analyze how the AFS-sets change for data set 2 if D is augmented by the pure concentration profile of the intermediate component of the chemical reaction (drawn in green in Fig. 8). The data augmentation is done as in (10) with $\gamma = 0.1 \max(D)/\max(c)$. The additional column of D leads to an additional constraint for $\mathcal{F}_S$. The modified polygon $\mathcal{F}_S$ is now the intersection of $n + 1$ affine half-spaces instead of only n ones. In fact, this additional constraint has a significant, size-decreasing impact on $\mathcal{F}_S$. The results are presented in Fig. 14. Now the two AFS-sets each have three separated subsets. Further, two subsets of the spectral AFS are line-shaped due to the additional restriction on $\mathcal{F}_S$. This result is consistent with the underlying duality relations [40, 26, 27]. Only $n^* = 12$ frequency channels are relevant for the augmented data instead of $n^* = 71$ for the original data.

6. Conclusion

The intrinsic uncertainty of the pure component factors of MCR decompositions is a major obstacle in the chemometric analysis of spectroscopic data. The *data-based ambiguity* [6, 29] locates the reason of this ambiguity in the

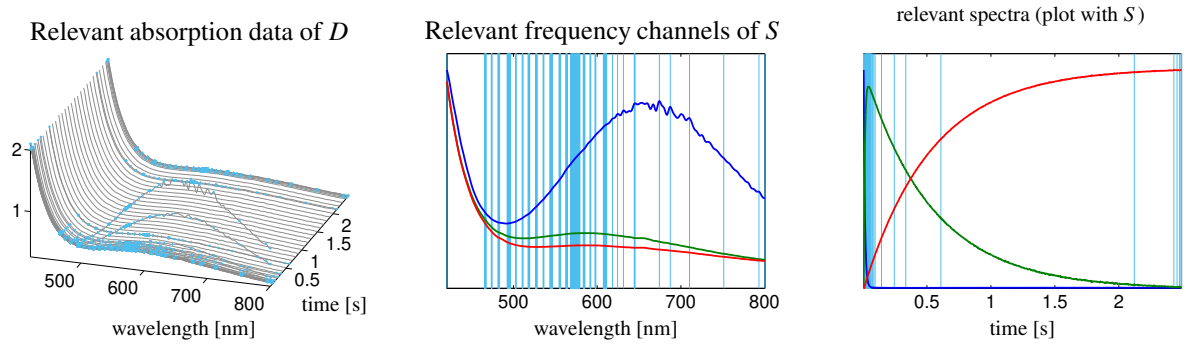

Figure 12: A posteriori redundancy analysis for the data set 2. Only $n^* = 71$ frequency channels (cyan lines/areas) that have an impact on the polygons $\mathcal{F}_S$ and $\mathcal{I}_C$. Further, only $k^* = 25$ mixture spectra (the times of their measurements are marked by vertical lines in cyan) have an impact on the polygons $\mathcal{F}_C$ and $\mathcal{I}_S$. The control parameter on the acceptance of small negative entries of C and S is $\varepsilon = 2.5 \cdot 10^{-3}$.

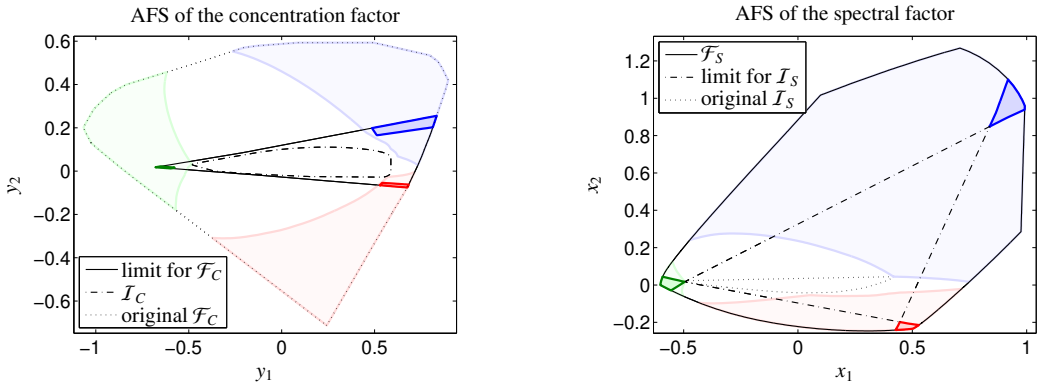

Figure 13: Data set 1: Computation of lower bounds on the the rotational ambiguity in the case of fixed pure component spectra. The reduced AFS-sets $\mathcal{M}_S$ and $\mathcal{M}_C$ representing the lower bounds on the ambiguity are drawn in colors. The original AFS-sets (transparent colors) are much larger. The intrinsic rotational ambiguity of the factorization is small but does not completely vanish. The remaining base level of ambiguity is caused by the fixed pure component spectra.

pure component factors. Hence a possible strategy for an ambiguity reduction is to modify the factor C of pure component concentration profiles in a proper way. The factor S is not often subject to change. The key elements of the theoretical analysis are of geometric nature, namely the polyhedra INNPOL and FIRPOL together with the simplex rotation algorithm. This algorithm rotates simplices *in* FIRPOL and *around* INNPOL in order to construct the set of feasible solutions.

Our main findings are that only some parts of the mixture spectra, namely primarily extremal points, have an impact on the AFS. This insight allows to formulate (loose) rules on how chemical experiments should be designed so that from spectral measurements reliable pure component information can be extracted. At the same time, some intrinsic base level of ambiguity appears to be unavoidable.

We hope that our analysis allows a deeper understanding of how MCR methods work and how to design a chemical experiment if an MCR analysis is intended. Spectral measurements taken in an appropriate manner can considerably influence the reliability of the results of chemometric analyses.

A. Mathematical background

The terms of reducibility/irreducibility of a symmetric matrix describe the zero pattern of a matrix [41]. The matrix elements of a reducible matrix can be permuted in a way that the permuted matrix has a block structure. For spectral data matrices reducibility can be often be interpreted in a way that the mixture data can be separated to independent chemical subsystems.

Definition A.1. *An $\ell \times \ell$ symmetric matrix A with $\ell \geq 2$ is called reducible, if an $\ell \times \ell$ permutation matrix P exists so that*

$$PAP^T = \begin{pmatrix} A_{1,1} & 0 \\ 0 & A_{2,2} \end{pmatrix}.$$

Therein $A_{1,1}$ is an $m \times m$ submatrix and $A_{1,2}$ is an $m \times (\ell - m)$ submatrix with $1 \leq m < \ell$. Otherwise, A is called an irreducible matrix.

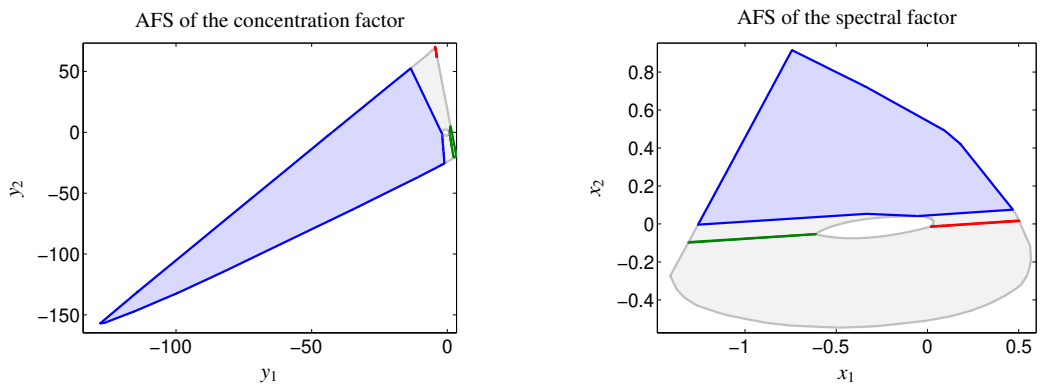

Figure 14: Data set 2: Reduction of the two AFS-sets by data augmentation of D by the concentration profile of the intermediate according to (10). The original AFS-sets are plotted in light gray, the reduced ones are colored. For both computations the joint basis of the SVD of the augmented spectral data matrix is used in order to compare the results.

References

[1] R.A. Fisher. The arrangement of field experiments. *Journal of the Ministry of Agriculture*, 33:503–513, 1926.

[2] R.A. Fisher. *The design of experiments.* Oliver & Boyd, Edinburgh, 1935.

[3] R. Tauler. Multivariate curve resolution applied to second order data. *Chemom. Intell. Lab. Syst.*, 30(1):133 – 146, 1995.

[4] R. Tauler, A. Smilde, and B. Kowalski. Selectivity, local rank, three-way data analysis and ambiguity in multivariate curve resolution. *J. Chemom.*, 9(1):31–58, 1995.

[5] R. Tauler, A. Izquierdo-Ridorsa, and Casassas E. Simultaneous analysis of several spectroscopic titrations with self-modelling curve resolution. *Chemom. Intell. Lab. Syst.*, 18(3):293 – 300, 1993.

[6] R. Manne. On the resolution problem in hyphenated chromatography. *Chemom. Intell. Lab. Syst.*, 27(1):89–94, 1995.

[7] M. Maeder and A. D. Zuberbühler. The resolution of overlapping chromatographic peaks by evolving factor analysis. *Anal. Chim. Acta*, 181(0):287–291, 1986.

[8] E. Malinowski. Factor analysis toolbox for Matlab. Applied Chemometrics, Inc., PO Box 100, Sharon, MA 02067, USA, 1992.

[9] O. M. Kvalheim and Y.-Z. Liang. Heuristic evolving latent projections: resolving two-way multicomponent data. 1. Selectivity, latent-projective graph, datascope, local rank, and unique resolution. *Anal. Chem.*, 64(8):936–946, 1992.

[10] P. Paatero, P.K. Hopke, X.-H. Song, and Z. Ramadan. Understanding and controlling rotations in factor analytic models. *Chemom. Intell. Lab. Syst.*, 60(1):253 – 264, 2002.

[11] P. Paatero and P.K. Hopke. Rotational tools for factor analytic models. *J. Chemom.*, 23(2):91–100, 2009.

[12] M. Garland. Combining operando spectroscopy with experimental design, signal processing and advanced chemometrics. State of the art and a glimpse of the future. *Catal. Today*, 155:266–270, 2010.

[13] M. Vosough, C. Mason, R. Tauler, M. Jalali-Heravi, and M. Maeder. On rotational ambiguity in model-free analyses of multivariate data. *J. Chemom.*, 20(6-7):302–310, 2006.

[14] M. Maeder and Y.M. Neuhold. *Practical data analysis in chemistry*. Elsevier, Amsterdam, 2007.

[15] H. Abdollahi and R. Tauler. Uniqueness and rotation ambiguities in multivariate curve resolution methods. *Chemom. Intell. Lab. Syst.*, 108(2):100–111, 2011.

[16] H. Schröder, M. Sawall, C. Kubis, A. Jürß, D. Selent, A. Brächer, A. Börner, R. Franke, and K. Neymeyr. Comparative multivariate curve resolution study in the area of feasible solutions. *Chemom. Intell. Lab. Syst.*, 163:55–63, 2017.

[17] O.S. Borgen and B.R. Kowalski. An extension of the multivariate component-resolution method to three components. *Anal. Chim. Acta*, 174:1–26, 1985.

[18] R. Rajkó and K. István. Analytical solution for determining feasible regions of self-modeling curve resolution (SMCR) method based on computational geometry. *J. Chemom.*, 19(8):448–463, 2005.

[19] A. Golshan, H. Abdollahi, and M. Maeder. Resolution of rotational ambiguity for three-component systems. *Anal. Chem.*, 83(3):836–841, 2011.

[20] M. Sawall, C. Kubis, D. Selent, A. Börner, and K. Neymeyr. A fast polygon inflation algorithm to compute the area of feasible solutions for three-component systems. I: Concepts and applications. *J. Chemom.*, 27:106–116, 2013.

[21] M. Sawall and K. Neymeyr. A fast polygon inflation algorithm to compute the area of feasible solutions for three-component systems. II: Theoretical foundation, inverse polygon inflation, and FAC-PACK implementation. *J. Chemom.*, 28:633–644, 2014.

[22] A. Jürß, M. Sawall, and K. Neymeyr. On generalized Borgen plots. I: From convex to affine combinations and applications to spectral data. *J. Chemom.*, 29(7):420–433, 2015.

[23] A. Golshan, M. Maeder, and H. Abdollahi. Determination and visualization of rotational ambiguity in four-component systems. *Anal. Chim. Acta*, 796(0):20–26, 2013.

[24] A. Golshan, H. Abdollahi, S. Beyramysoltan, M. Maeder, K. Neymeyr, R. Rajkó, M. Sawall, and R. Tauler. A review of recent methods for the determination of ranges of feasible solutions resulting from soft modelling analyses of multivariate data. *Anal. Chim. Acta*, 911:1–13, 2016.

[25] M. Sawall, A. Jürß, H. Schröder, and K. Neymeyr. *On the analysis and computation of the area of feasible solutions for two-, three- and four-component systems*, volume 30 of Data Handling in Science and Technology, "Resolving Spectral Mixtures", Ed. C. Ruckebusch, chapter 5, pages 135–184. Elsevier, Cambridge, 2016.

[26] R.C. Henry. Duality in multivariate receptor models. *Chemom. Intell. Lab. Syst.*, 77(1-2):59–63, 2005.

[27] R. Rajkó. Natural duality in minimal constrained self modeling curve resolution. *J. Chemom.*, 20(3-4):164–169, 2006.

[28] M. Sawall, A. Jürß, H. Schröder, and K. Neymeyr. Simultaneous construction of dual Borgen plots. I: The case of noise-free data. *J. Chemom.*, 31:e2954, 2017.

[29] R. Rajkó, H. Abdollahi, S. Beyramysoltan, and N. Omidikia. Definition and detection of data-based uniqueness in evaluating bilinear (two-way) chemical measurements. *Anal. Chim. Acta*, 855:21 – 33, 2015.
[30] M. Sawall, A. Moog, C. Kubis, H. Schröder, D. Selent, R. Franke, A. Brächer, A. Börner, and K. Neymeyr. Simultaneous construction of dual Borgen plots. II: Algorithmic enhancement for applications to noisy spectral data. *J. Chemom.*, 32:e3012, 2018.
[31] W.H. Lawton and E.A. Sylvestre. Self modelling curve resolution. *Technometrics*, 13:617–633, 1971.
[32] H. Laurberg, M.G. Christensen, M.D. Plumbley, L.K. Hansen, and S.H. Jensen. Theorems on Positive Data: On the Uniqueness of NMF. *Computational Intelligence and Neuroscience*, 2008:9 pages, 2008.
[33] S. Beyramysoltan, R. Rajkó, and H. Abdollahi. Investigation of the equality constraint effect on the reduction of the rotational ambiguity in three-component system using a novel grid search method. *Anal. Chim. Acta*, 791(0):25–35, 2013.
[34] E.R. Malinowski. Window factor analysis: Theoretical derivation and application to flow injection analysis data. *J. Chemom.*, 6(1):29–40, 1992.
[35] H.R. Keller and D.L. Massart. Evolving factor analysis. *Chemom. Intell. Lab. Syst.*, 12(3):209–224, 1991.
[36] C. Kubis, M. Sawall, A. Block, K. Neymeyr, R. Ludwig, A. Börner, and D. Selent. An operando FTIR spectroscopic and kinetic study of carbon monoxide pressure influence on rhodium-catalyzed olefin hydroformylation. *Chem.-Eur. J.*, 20(37):11921–11931, 2014.
[37] T. Beweries, C. Fischer, S. Peitz, V. V. Burlakov, P. Arndt, W. Baumann, A. Spannenberg, D. Heller, and U. Rosenthal. Combination of spectroscopic methods: In situ NMR and UV/Vis measurements to understand the formation of group 4 metallacyclopentanes from the corresponding metallacyclopropenes. *J. Am. Chem. Soc.*, 131(12):4463–4469, 2009.
[38] C. Fischer, T. Beweries, A. Preetz, H.-J. Drexler, W. Baumann, S. Peitz, U. Rosenthal, and Heller D. Kinetic and mechanistic investigations in homogeneous catalysis using operando UV/Vis spectroscopy. *Catal. Today*, 155(3–4):282–288, 2010.
[39] M. Sawall, C. Kubis, E. Barsch, D. Selent, A. Börner, and K. Neymeyr. Peak group analysis for the extraction of pure component spectra. *J. Iran. Chem. Soc.*, 13(2):191–205, 2016.
[40] M. Sawall, C. Fischer, D. Heller, and K. Neymeyr. Reduction of the rotational ambiguity of curve resolution techniques under partial knowledge of the factors. Complementarity and coupling theorems. *J. Chemom.*, 26:526–537, 2012.
[41] R.S. Varga. *Matrix Iterative Analysis*. Springer Series in Computational Mathematics. Springer Berlin Heidelberg, 1999.